On the role of kinking in the bearing failure of composite laminates

Cyril Sola [a,b,*], Bruno Castanié [b], Laurent Michel [b], Frédéric Lachaud [b], Arnaud Delabie [a], Emmanuel Mermoz [a]

[a] Drive Systems Department, Airbus Helicopters, Aéroport Marseille-Provence, 13725 Marignane Cedex, France
[b] Groupe Matériaux et Structures Composites (MSC), Université de Toulouse, FRE CNRS 3687, INSA/UPS/ISAE/Mines Albi, Institut Clément Ader, 3 Rue Caroline Aigle, 31400 Toulouse, France

Keywords:
Composite
Laminate
Bearing
Kinking
Compression
Non-local

A B S T R A C T

Fibre kinking is one of the main failure modes of composite laminates under compression loading. In this paper, the role of kinking in the failure of quasi isotropic composites subjected to a bearing load is inves tigated. High resolution CT scans show that kinking is largely involved in the events leading to laminate collapse, notably by triggering other damage modes such as delamination. Kink bands develop extremely progressively, leading to the formation of a wide localization zone (or FPZ, failure process zone). Such behaviour calls for a non local modelling approach. Local damage models would lead to overly conserva tive sizing. A simple model, based on Hashin failure criteria and non local effective stresses is confronted to experiments, and its limits are highlighted. It will be shown that proper modelling of the bearing fail ure requires the characteristic behaviour of kink bands to be taken into account.

1. Introduction

Bearing failure has been widely studied, both experimentally and numerically [1]. However, the complex nature of this failure mode still makes it a challenging test case for damage models [2]. Most experimental studies have focused on the bearing beha viour of pinned or bolted composite joints, with typical bearing strength (Eq. (1)) ranging from 400 MPa to 1000 MPa.

$$\sigma_{bearing} \quad \frac{F}{t \cdot d} \tag{1}$$

Thus, the boundary conditions pertaining to each joint configu ration appear to have considerable influence on the bearing strength. The most influential ones are the lateral restraint due to bolt preloading [3], the bolt hole clearance [4], or secondary bending for single lap shear joints. The damage mechanisms involved in the bearing failure of bolted joints have been studied by Xiao and Ishikawa [5], who showed that kinking (often referred to as fibre microbuckling) plays an important role in the failure process, as did Seike et al. [6]. Camanho et al. [7] showed that the progressiveness of the bearing failure could be explained by the accumulation of subcritical damage. They emphasised the role of delamination, suggesting the use of three dimensional failure criteria, which they did in a later paper [8]. However, cohesive zone models do not seem to be an absolute requirement [9]. Despite the many models proposed in the literature, which are often based on traditional failure criteria [8,10 12], the sizing of composite joints is still mainly based on allowable bearing strengths obtained for different joint configurations.

Hence, there still is a need for improved failure models built upon a sound physical basis. Mutual feedback should be estab lished between the numerical models and the experiments to look beyond the load displacement curve. To do this, it would be desir able to use very simple experiments, such as pinned contact [13] or half hole pinned bearing [14 17], in order to reduce the number of unknown or uncertain variables and to focus on the damage mech anisms. A more general knowledge of the bearing failure would also make it possible to diverge from the traditional bolt/rivet mechanical assemblies in specific industrial applications.

In this paper, bearing failure and the role of kinking are further investigated using a half hole pinned bearing test and modern experimental techniques such as computed tomography (CT) and digital image correlation (DIC), for both woven and UD fabric lam inates, with the same epoxy matrix. An enhanced engineering fail ure model is then introduced, exhibiting large similarities with most of the existing failure theories dedicated to bearing failure simulation. The enhancement mainly stems from the use of an embedded non local approach, which prevents an excessive impact of subcritical damage on the failure load. However, the aim of this paper is less to propose a new failure theory than to point out the deficiencies of such theories, and to suggest other

* Corresponding author at: Drive Systems Department, Airbus Helicopters, Aéroport Marseille-Provence, 13725 Marignane Cedex, France.

http://dx.doi.org/10.1016/j.compstruct.2016.01.058

modelling strategies based on the observed damage mechanisms, with a special emphasis on kinking, which will be shown to play a prominent role. The need for advanced damage models dedicated to the compressive failure of composite materials will be highlighted.

2. Experimental study

2.1. Experimental procedure

To study the intrinsic bearing behaviour, it was decided to carry out half hole bearing tests. One of the main advantages associated with this kind of test is the fact that the full strain field on the free surface of the laminate can be obtained using digital image correlation (DIC). The small coupon size and the simple test set up (Fig. 1) both help to render experiments simpler to analyse and models faster to run. The gauge length can be made arbitrarily small, so that global buckling problems are avoided.

The indenter, or "pin", was the aft part of a ϕ 6.35 mm Diager reamer, of the same type as the one used to ream holes after a three step drilling process.

Two types of prepregged fabrics with the same resin system were chosen: a UD fabric and a 4 harness satin weave (Fig. 2). The tows were made of 3 k HTA fibres, and the thermoset resin was a second generation toughened epoxy.

A quasi isotropic layup $[90, +45, 0, \ \ 45]_{ns}$ was selected for both materials. The number of stacking sequences, n, was determined so as to obtain panels of similar thickness, which were laid up by hand and cured in a press, at 180 °C under a pressure of 4 bars. The UD fabric laminates were 4 mm thick and the woven fabric laminates 3.75 mm thick.

An INSTRON 250 kN machine was used for the static tests. As strain softening was expected, tests were run under displacement control, with a displacement rate of 0.2 mm/min. A VIC 2D digital image correlation system was used, with an AVT Pike F505B camera having a resolution of 2452 × 2452 pixels. Stereo correlation was not deemed necessary as the coupon mainly deformed in plane when not heavily damaged.

Three static tests were performed for both materials.

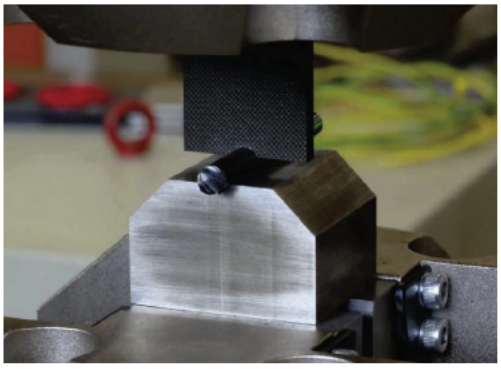

Fig. 1. Half-hole pinned bearing coupon and test set-up.

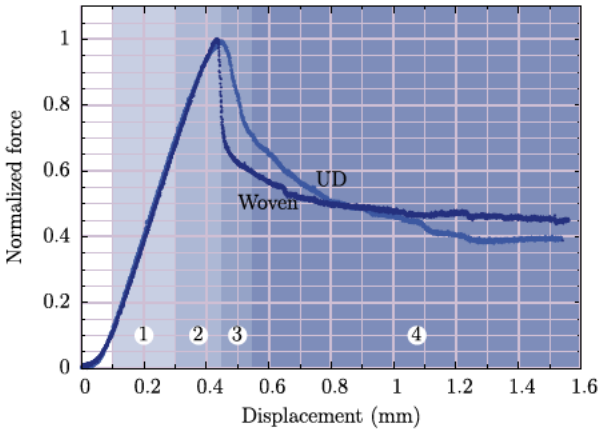

Fig. 3. Typical force–displacement data points for woven and UD-fabric laminates, with a quasi-isotropic layup.

2.2. Macroscopic bearing behaviour

The load displacement curve (Fig. 3) showed four main behaviours and was repeatable.

1. The first part was essentially linear, except for the very beginning, where the non linearity could be attributed to the existence of a small perpendicularity defect (<1°), as revealed by a careful analysis of DIC results. The initial non linearity could not be explained by varying contact conditions in relation with clearance, since the hole and the indenter had the same diameter.
2. At about 70% of the peak strength, the load displacement relationship became slightly non linear.
3. Just after the peak strength, a sharp load drop occurred, accompanied by a loud cracking noise.
4. As displacement increased, the load then stabilized and oscillated around a residual value approximately equal to 40% of the peak strength, and it continued to do so even for displacement magnitudes of the same order as the hole radius. It was noted that this proportion was identical for UD fabric and woven fabric laminates.

The failure point was easy to define, as a sharp load drop occurred just after the peak strength. Hence, there was no need to define a bearing failure strain, though this is defined in most

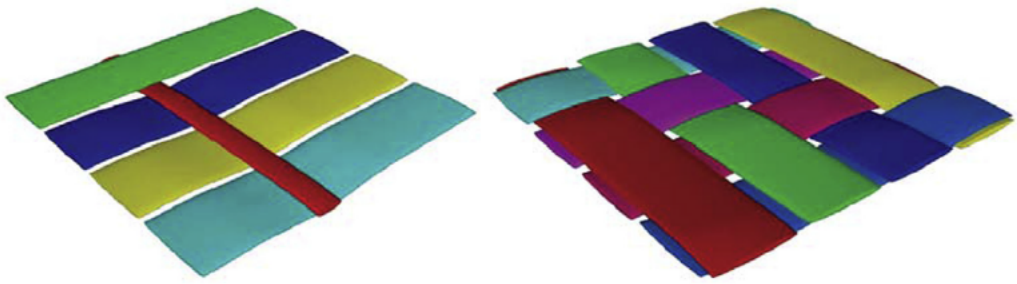

Fig. 2. Architectures of the UD (left) and woven (right) fabrics. The UD-fabric contains a small proportion of weft glass yarns.

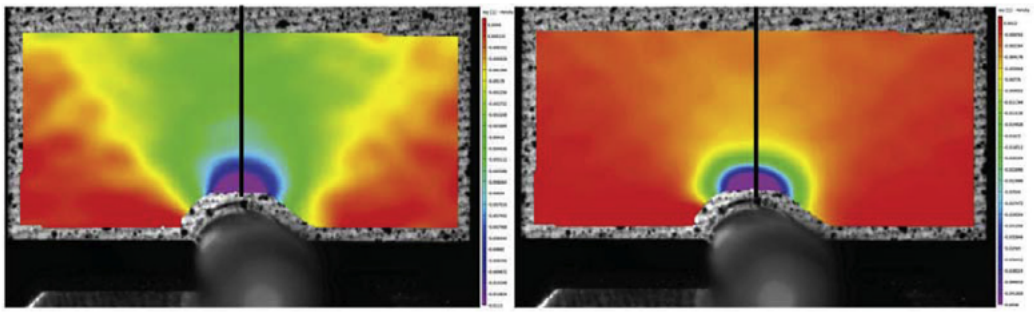

Fig. 4. Pre-peak and post-peak strain fields obtained by DIC. The strain profiles on Figs. 6 and 5 are extracted along the black line.

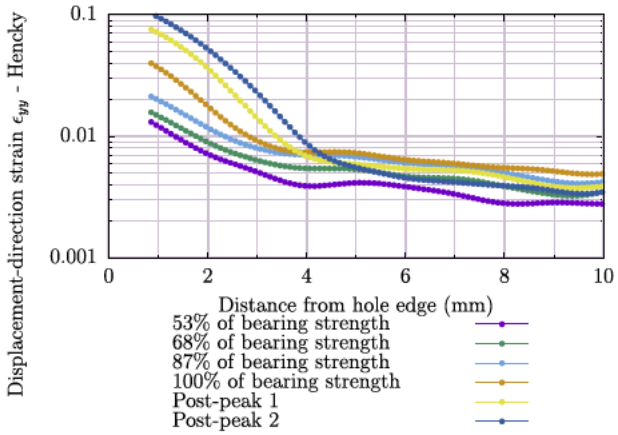

Fig. 5. Evolution of the displacement-direction strain profile for a UD-fabric laminate with increasing displacement. Note that, once the bearing peak is passed, unloading occurs beyond about 4 mm from the hole edge, denoting damage localization. The vertical axis has a logarithmic scale.

engineering connections failing in bearing, and is typically equal to 4% of the hole diameter as recommended by ASTM D953 37. The estimated COV[1] on the peak strength value was extremely small, lower than 2% for both materials. Woven and UD fabric laminates had almost the same bearing strength, with a slight advantage for the bidirectional weave architecture (+6%). The more sudden drop in load carrying capability in the woven laminates could be attributed to the failure of the lower and upper plies. Unlike the corresponding plies in the UD fabric laminates, these plies contained 0° weft yarns. Since they did not benefit from ply constraint effects, they tended to fail at lower loads than inner plies. As these yarns accounted for 25% of the 0° oriented yarns, their failure had a strong effect on the global response.

Further information could be obtained thanks to DIC. This technique enabled the strain field variations to be followed as the load increased (Figs. 4 and 5). No obvious localization was observed before peak strength. However, in the UD fabric laminates, the displacement direction strain levels could be rather high, largely above 1.1%, which is accepted as the compressive failure strain of the fibres. Assuming these strains were almost constant through the thickness, which should be true as long as there is sufficient cohesion between the plies, it can be concluded that failure in the fibre direction initiated before peak strength, explaining the observed non linear behaviour. In the woven fabric laminates, strain levels appeared to be more erratic, as load was redistributed at a larger distance from the hole edge. An increase in the resolution showed that high local strains also existed before peak strength.

At the bearing peak, the displacement direction strain profile along a line located on the geometric longitudinal symmetry plane was remarkably similar for all the UD fabric specimens (Fig. 6). However, in the woven fabric laminates, the strain profiles for coupons failing at similar loads were not alike. The weave architecture significantly influenced the local strain levels, which oscillated. In addition, the surface strain field was altered by the joint presence of 0° and 90° yarns.

After the bearing peak, strains quickly became localised in a zone whose size did not seem to change much with increasing displacement. All the material points located outside this zone were progressively less and less strained while strain levels soared in the FPZ (Failure Process Zone). This is particularly noticeable on Fig. 5, where, after the bearing peak, strain levels tend to decrease beyond a distance from the hole edge roughly equal to 4 mm. In fact, beyond the bearing peak, the coupons behaved as if they were composed of two very different materials: a "soft" one (heavily damaged composite) in the FPZ, and a "hard" one (pristine composite) outside.

One of the key difficulties associated with the use of digital image correlation software is the choice of the correlation parameters, namely the subset size, the step size, and the filter size used for strain computations. These three parameters define the so called "virtual strain gauge size". By modifying them, it was shown that strain levels could vary over a large range. Nevertheless, they were consistently of the order of several percent, unless the virtual strain gauge size was increased to several millimetres or the strain field was abusively filtered. This was even the case before the peak strength, so it could be inferred that fibre failures occurred before

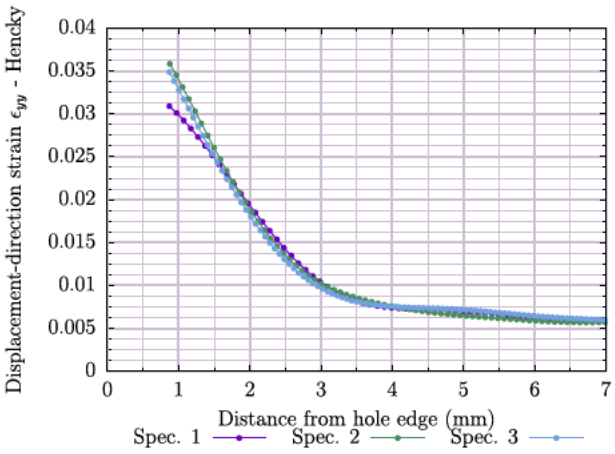

Fig. 6. Displacement-direction strain profile for three UD-fabric specimens at bearing peak.

[1] Coefficient of variation.

this point was reached. Of course, when strain gradients are mild, these parameters have a much smaller influence on the computed strains. This could be checked by numerically and homogeneously deforming a picture of a coupon with a speckle pattern.

2.3. Ply scale bearing behaviour

Tests were stopped at various times to obtain coupons with different damage levels for further analysis using computed tomography. Regarding the very low COV on the bearing strength and the almost identical strain profiles, it could be considered that all the coupons experienced the same damage kinetics. Therefore, there was no need for *in situ* tomography. The main range of interest was between about 70% and 100% of the bearing strength, i.e. where the load displacement relationship was non linear. The resolution performance of computed tomography is highly dependent on the ratio of distances between the X ray source and the specimen on the one hand, and between the source and the detector array on the other. As a general rule, the closer the specimen is to the source, the better is the resolution. Therefore, coupons were cut to a smaller size, leaving a minimal distance of about two millimetres between the hole edge and the slice boundary. They were CT scanned in a GE Phoenix VTome XM microtomograph. With 3000 frames, the full reconstruction took about one hour per coupon. In the end, a very acceptable resolution of about 4 µm was obtained.

Coupons obtained after tests stopped at about 70% of the peak strength were not seriously damaged. However, matrix cracks were present, mainly in the upper and lower plies. More interesting was the presence of small kink bands initiating from the very edge of the hole. They were hardly visible, but were present in load bearing plies, namely the 0° and ±45° plies, in the upper and lower ply sequences. Unfortunately, the contrast of these images (not shown) was very poor, making the kink bands difficult to pinpoint. At a slightly higher load level (80% of the peak strength), kink bands continued to develop in the upper and lower ply sequences, and started to develop and multiply in the inner ply sequences, up to the bearing peak. Figs. 7 and 8 show typical kink bands in a UD fabric laminate, and Fig. 9 shows kink bands in a woven fabric laminate. Fig. 10 shows kink bands in a 45° ply. Kink bands propagated in plane (along the width of the laminate) and out of plane (through the thickness of the laminate). They could cross several plies of different orientation without changing their in plane direction of propagation, hence creating through thickness failure surfaces. Some authors have referred to such damage as "out of plane shear cracks", but it seems that these bands really are related to kinking (Fig. 11), thus deserving the name "kink bands". In some cases, kink bands terminate in longitudinal matrix cracks (*splitting*), see Fig. 9.

Through thickness failure planes created wedge mechanisms at several locations in the laminate, leading, upon further loading, to delaminations (Fig. 12). Most of the delaminations did not initiate from the hole wall, as they would have if they had initiated on their own, but from inside the laminate. Therefore, in most cases, kinking triggered delaminations, and not the opposite. In the $[90, +45, 0, \ 45]_{ns}$ laminates of this study, delaminations were mainly located in the lower and upper ply sequences. The absence of noticeable delaminations in the central sequences was probably the consequence of ply constraint effects (stacking sequence effects) which have been shown to have considerable influence on delamination bearing strength [18]. Another important element is that a compressive out of plane normal stress exists, due to friction between the composite and the indenter limiting the laminate expansion. The same facts probably also explain why kink bands tended to extend more deeply inside the laminate in the central ply sequences. By preventing out of plane motion, the load aligned yarns could be further strained, thus creating other kink bands.

It is thought that the load drop following the bearing peak is due to the motion of the different wedge mechanisms, triggering multiple delaminations. The role of these wedges in the final failure has already been discussed by Hirano et al. [16]. It appears that

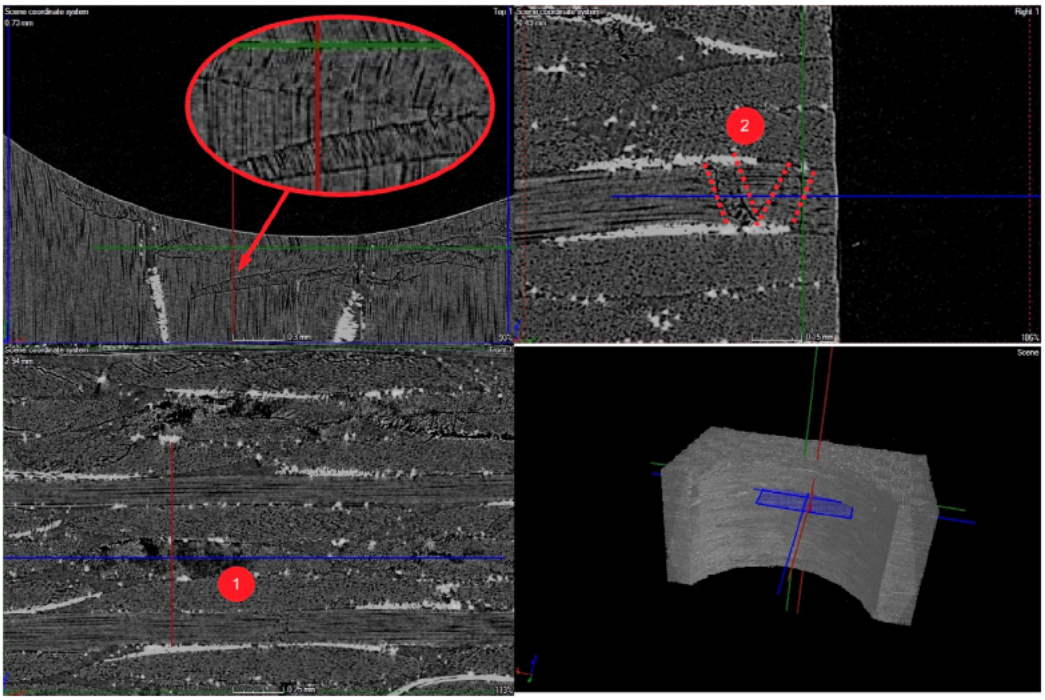

Fig. 7. Kink bands viewed from different perspectives in a UD-fabric laminate at bearing peak. On the bottom left image, black areas (1) correspond to cracked surfaces delimiting kink bands. On the top right image, note the characteristic chevron shape (2) due to the reflection of a kink band, probably triggered by the presence of flame retardant particles (white dots, which should not be confused with transverse glass yarns).

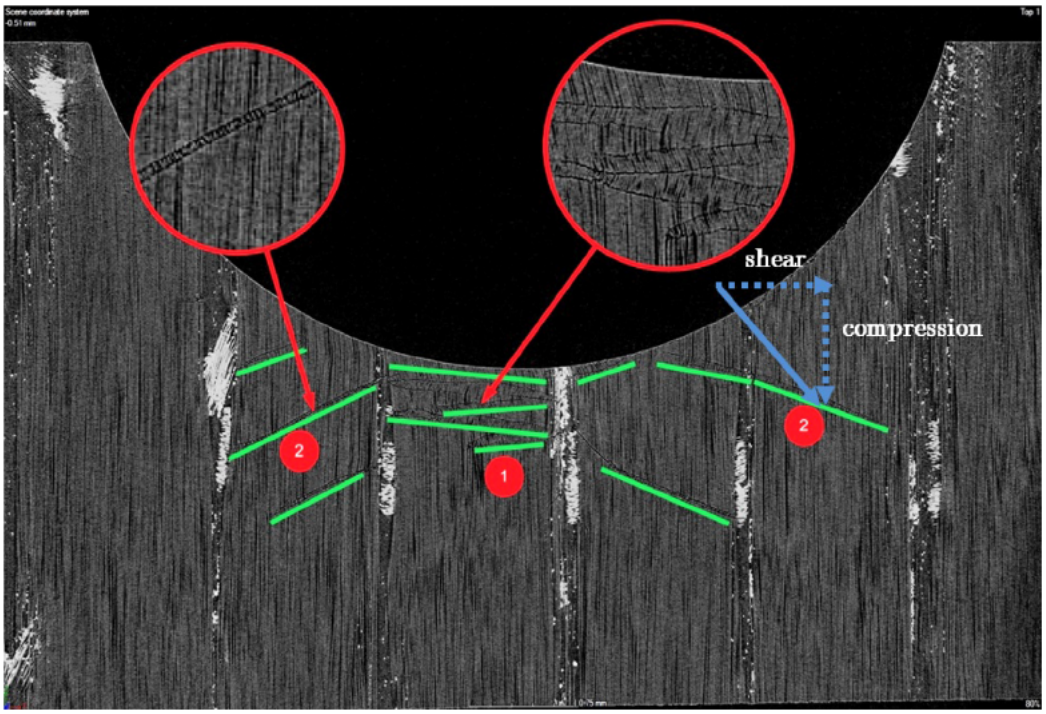

Fig. 8. Kink bands in a 0° ply (UD-fabric laminate) at bearing peak. Their in-plane direction of propagation depends on their location. Kink bands located in zones where both compressive and shear strains are high (2) are tilted with respect to the loading direction, while kink bands located in the frontal zone (1) are perpendicular to it. This shows that kink band initiation and propagation is not only sensitive to compressive strains, but also to shear strains.

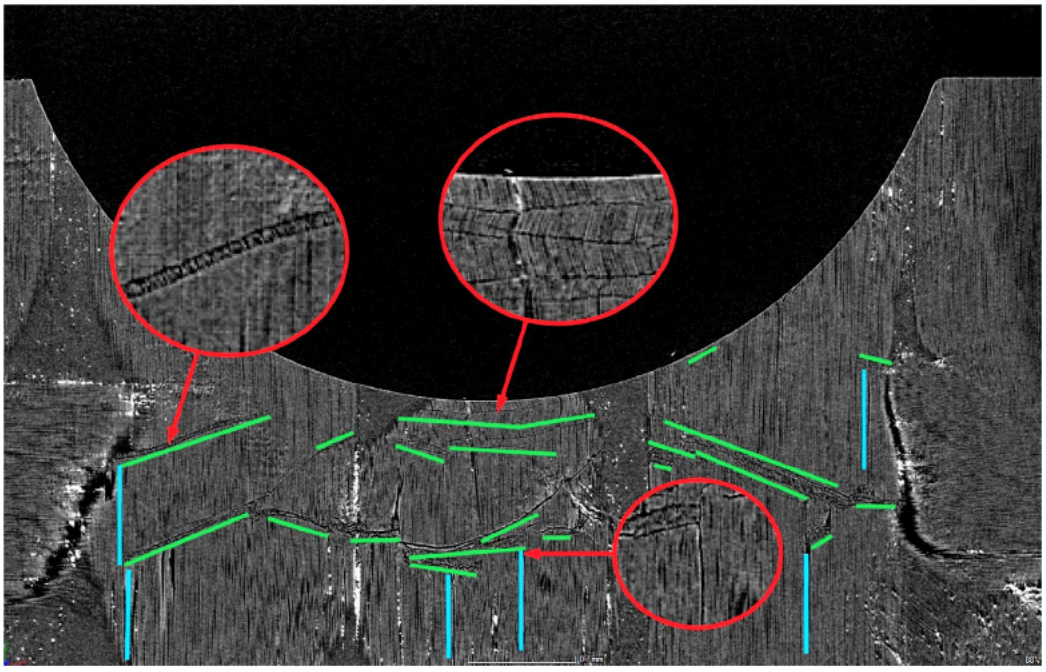

Fig. 9. In this woven fabric ply with 0° warp yarns, multiple kink bands can be observed when the bearing peak is reached. Some splitting cracks can be noticed (in cyan). (For interpretation of the references to colour in this figure legend, the reader is referred to the web version of this article.)

woven laminates are also prone to delamination, and especially inter yarn debonding, the wedge mechanism also being involved.

Hence, kinking appears to play a central and dominant role in the events leading to laminate collapse. This idea is further rein forced by the great similarity between the macroscopic response of laminates loaded in bearing and that of unidirectional notched laminates subjected to a compressive load, which fail as a conse quence of kink band propagation [19].

These observations also suggest that the high strain levels before peak strength was reached could be related to the existence of numerous kink bands spanning the whole thickness of the lam inates and having a width comparable to the diameter of the hole.

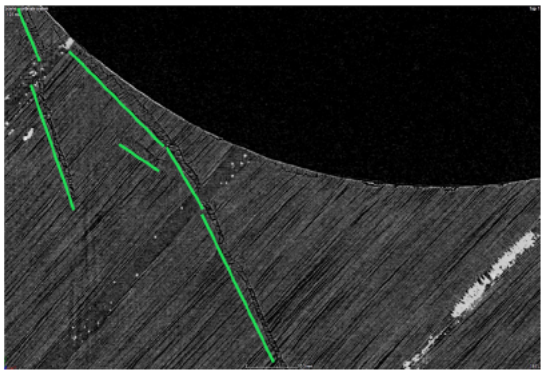

Fig. 10. Kink bands can be found in ±45° plies when the peak strength is reached, but also before, in both UD-fabric (this picture) and woven fabric laminates.

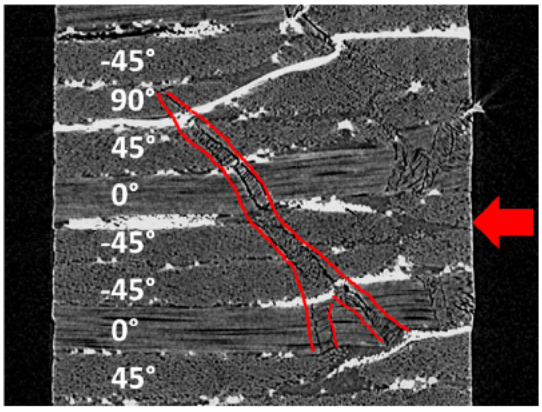

Fig. 11. Kink bands can propagate out of plane and through other plies (UD-fabric laminate) by some sort of domino effect, but it is almost impossible for them to cross a 90° ply.

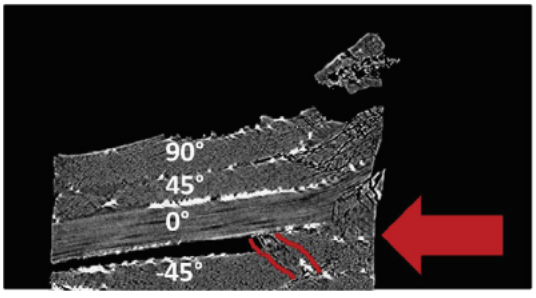

Fig. 12. Detail showing a wedge mechanism inducing a delamination. Although this coupon failed in a low cycle fatigue test, this type of interaction between kinking and delamination has also been observed under static loads.

3. A simple non-local failure model for UD-fabric laminates

3.1. Theory and model

Non local damage models were firstly developed for concrete, but more generally, they apply to materials termed "quasi brittle", i.e., materials that are characterised by their ability to dissipate a lot of energy before reaching their peak strength, essen tially by diffuse microcracking in a zone that can be of non negligible dimensions with respect to the structure size (at the lab scale). They can be used to simulate size effects, which are related to the transition from a strength controlled ductile beha viour at small scales to a fracture toughness controlled brittle behaviour at larger scales. The main characteristic non local mod els have in common is that they incorporate an internal length, that has some sort of physical meaning, as Bažant demonstrated [20]. The average stress and point stress failure criteria of Whitney and Nuismer are forms of "non local" approaches, as is the Failure Characteristic Volume (FCV) of Hochard [21]. The underlying idea is that an interaction exists between material points located in a small volume so that, from the material perspective, the strain sin gularity close to a crack or a hole can be partially relieved. In addi tion, in a continuum damage mechanics (CDM) framework, the internal length prevents spurious localization by controlling the size of the zone that undergoes softening. Spurious localization is related to the loss of uniqueness of the boundary value problem, which is a consequence of softening. In a finite element model, this means that the number of possible unloading paths at each inte gration point is potentially infinite. In some extreme cases, snap back could occur, resulting in insufficient or virtually zero energy dissipation in case of complete snap back to the origin of the load displacement graph.

As kinking generates a size effect in notched laminates [22], and as bearing failure has been seen to be associated with a large FPZ, with the first kink bands developing before peak strength and act ing as microcracking, it seems reasonable to consider a non local approach when modelling this kind of failure.

The model proposed here is based on three dimensional Hashin criteria and requires only common material data. The failure crite ria are associated with four failure modes, namely:

- Tensile fibre failure if $\sigma_{11} \geqslant 0$

$$\left(\frac{\sigma_{11}}{X_{T,1}}\right)^2 + \frac{\sigma_{12}^2 + \sigma_{13}^2}{S_{12}^2} \quad 1 \tag{2}$$

- Compressive fibre failure if $\sigma_{11} < 0$

$$\frac{\sigma_{11}}{X_{C,1}} \quad 1 \tag{3}$$

- Tensile matrix failure if $(\sigma_{22} + \sigma_{33}) > 0$

$$\left(\frac{\sigma_{22} + \sigma_3}{X_{T,2}}\right)^2 + \left(\frac{\sigma_{23}^2 \quad \sigma_{22}\sigma_{33}}{S_{23}^2}\right) + \frac{\sigma_{12}^2 + \sigma_{13}^2}{S_{12}^2} \quad 1 \tag{4}$$

- Compressive matrix failure if $(\sigma_{22} + \sigma_{33}) < 0$

$$\frac{1}{X_{C,2}} \quad \left(\frac{X_{C,2}}{S_{12}}\right)^2 \quad 1\Bigg)(\sigma_{22} + \sigma_{33}) + \frac{1}{4}\left(\frac{\sigma_{22} \quad \sigma_{33}}{S_{23}}\right)^2 + \frac{\sigma_{23}^2 \quad \sigma_{22}\sigma_{33}}{S_{23}^2} + \frac{\sigma_{12}^2 + \sigma_{13}^2}{S_{12}^2} \quad 1 \tag{5}$$

These criteria are used to trigger damage. Each of them is related to a damage variable. Once a failure is detected, the corre sponding damage variable instantaneously increases from 0 to a value very close to 1 (typically 0.99).

To ease the convergence process of the implicit algorithm once damage has initiated, a delayed damage model is implemented. This model, similar to viscous regularization schemes, introduces a time constant τ, which limits the damage evolution rate [23]. The shape parameter a is set equal to one. Limiting the damage evolution rate allows elements that are not in the boundary layer to be further strained, and possibly damaged, before the global unloading ("strain softening") starts.

$$\dot{d}_r \quad \frac{1}{\tau}(1 \quad \exp(\ a(d \quad d_r)) \tag{6}$$

The damage variables are then replaced by their regularized counterparts.

$$\begin{array}{ll} d_{ft} & d_{r,ft} \\ d_{fc} & d_{r,fc} \\ d_{mt} & d_{r,mt} \\ d_{mc} & d_{r,mc} \end{array} \tag{7}$$

These damage variables are then condensed into two damage variables, related to fibre damage or to matrix damage. They will be used to translate the effect of damage on the compliances. No specific damage variable is used to model shear behaviour. This simplified approach is similar to that proposed by Gutkin and Pinho [24].

$$d_f \quad \max(d_{ft}, d_{fc}, d_f^N) \tag{8}$$

$$d_m \quad \max(d_{mt}, d_{mc}, d_m^N) \tag{9}$$

The superscript N refers to the previous converged iteration. This definition of damage ensures that damage can only increase or remain stable once it has initiated.

The damaged compliance matrix then reads:

$$\widetilde{S} \quad \begin{bmatrix} \frac{1}{E_1(1\ \ d_f)} & \frac{\nu_{12}}{E_1} & \frac{\nu_{13}}{E_1} & 0 & 0 & 0 \\ \frac{\nu_{12}}{E_1} & \frac{1}{E_2(1\ \ d_m)} & \frac{\nu_{23}}{E_2} & 0 & 0 & 0 \\ \frac{\nu_{13}}{E_1} & \frac{\nu_{23}}{E_2} & \frac{1}{E_3(1\ \ d_m)} & 0 & 0 & 0 \\ 0 & 0 & 0 & \frac{1}{G_{12}(1\ \ d_m)} & 0 & 0 \\ 0 & 0 & 0 & 0 & \frac{1}{G_{23}(1\ \ d_m)} & 0 \\ 0 & 0 & 0 & 0 & 0 & \frac{1}{G_{13}(1\ \ d_m)} \end{bmatrix} \tag{10}$$

Its inverse, the stiffness matrix, is also the tangent operator, since damage evolution is not related to stresses or strains.

In the proposed model, stresses in the failure criteria are replaced by effective stresses after the initiation of damage:

$$\sigma_{ij} \quad \tilde{\sigma}_{ij} \tag{11}$$

where $\sigma_{ij} \quad \frac{\sigma_{ij}}{1\ \ d_f}$ if $i \quad j \quad 1$ and $\sigma_{ij} \quad \frac{\sigma_{ij}}{1\ \ d_m}$ if $i,j \in [2,3]$.

Non local enhancement. The non local approach is used to eval uate the failure criteria in a non local way, much as in the FCV method proposed Hochard and coworkers [21]. The FCV approach is built upon an external subroutine because a user material model is not able to handle several integration points simultaneously (the routine loops through every integration point in a sequential way). In the current model, the procedure can be directly embedded in the finite element code by using the non local capabilities of Sam cef,[2] which makes it possible to establish a "dialogue" between neighbouring Gauss points. Using the built in implicit gradient model, it is possible to compute non local variables in a user mate rial routine by simply enhancing the stress vector and the tangent matrix. In contrast with the FCV, the implicit gradient enhanced approach is not a simple averaging, but a weighted average similar to the Gaussian averaging of traditional integral non local approaches [25]. In fact, the implicit gradient enhanced model is a diffusion equation, relating a local variable f to its non local counter part $\bar{f}$ and involving an internal length c. It is associated with an equation enforcing zero flux at the boundaries of the material domain considered, Ω, which ensures that a homogeneous field remains unchanged.

$$\begin{cases} f \quad c^2\Delta f \quad f & \text{in} \quad \Omega \\ \vec{\nabla} f.\vec{n} \quad 0 & \text{on} \quad \partial\Omega \end{cases} \tag{12}$$

Samcef allows only one internal length to be used. Thus, the internal length cannot be fine tuned to each damage mode, which would be preferable [26].

The fact that damage is instantaneous, denoting *perfectly brittle* behaviour, might seem to contradict the idea that damage should be non local to simulate the *quasi brittle* nature of composite materials. In fact, in this model, the non local approach, applied to the failure criteria only, is used as a simple way of emulating the effect of the progressive failure without actually needing a complete set of unconventional material parameters, which are tricky to identify and most often not available to the engineer at the design stage.

In the non local approach, effective stresses σ are replaced by the effective non local stresses $\bar{\sigma}$ when evaluating failure criteria. Non local averaging can be applied to any component of the stress tensor. Alternatively, non local strains could be computed. The constitutive relation between stresses and strains remains local, which preserves the original elastic behaviour.

3.2. Results

A typical coupon was modelled using hexahedral elements, with one layer of elements per ply in the refined zone of interest. The pin was assumed to be perfectly rigid, which improved calcu lation times while providing results very close to a flexible/flexible contact. The friction coefficient was taken to be equal to 0.1. This value was selected on the basis of an analysis of the DIC results focusing on the shapes of the different strain fields (shear and transverse strains in particular). It has no direct physical meaning, and should merely be seen as an average of the local friction coef ficients, which would vary depending on the local angle between the fibres and the slip directions.

Local model. The local model predicts a peak strength that is much lower than the actual one. Since damage almost instanta neously increases to 0.99, the laminate has no further possibility to absorb (by deforming elastically) or dissipate (by failing pro gressively) strain energy, and it thus fails immediately.

It should be noted that in the model proposed by Camanho and Matthews [8], which is based on the same failure criteria as the current model, damage is deemed to have much less influence on the components of the damaged stiffness tensor. For example, the fibre stiffness would only decrease by 86% upon failure initia tion under compression, whereas in the present model, the dam aged stiffness is virtually reduced to 0 when damage is total. While, regarding stiffness, Camanho's approach is probably closer to reality, as compressive damage appears unlikely to lead to a complete stiffness loss, its major drawback is that it enables con siderable energy storage in the laminate, since non completely damaged elements would continue to load elastically. Whether this energy storage is real or artificial remains to be debated, espe cially when one considers the kink band broadening phenomenon, which supposedly takes place at constant stress. What is certain is that such an approach, although physically motivated, greatly delays the numerical peak strength, which can even be non existent (Fig. 14).

Non local model. The non local model delays initiation depend ing on the internal length value, effectively limiting the impact of the first subcritical damage on the failure load by simply ignoring it. It was found that, to obtain a numerical peak strength close to the experimental value, the model should be fully non local, mean ing that all the failure criteria should be evaluated using non local effective stresses, with a very large internal length of 1.5 mm.

[2] FEA package commercialised by Siemens.

Such a large internal length produces several effects that make the model's response physically unrealistic:

1. The damaged zone associated with fibre compressive damage is much too large (Fig. 13) compared to the actual zone (see Fig. 8 for example).
2. There is no matrix damage at the bearing peak, which contra dicts the experimental evidence. Due to the large internal length, matrix damage is effectively considered as subcritical.
3. $\pm 45^{\circ}$ plies are not damaged, whereas the CT scans revealed that kink bands appeared in these plies long before peak strength was reached, just like in 0° plies.
4. By delaying the initiation, this non local model is not able to represent the physical reality, i.e., the fact that kinking starts quite soon but then develops progressively. In particular, the non linearity preceding the bearing peak cannot be represented (Fig. 14). Although this is a natural consequence of using non local failure criteria, the large internal length introduces such a delay between the real initiation load and the simulated one that it might have serious consequences on the failure scenario in some cases. Hence, the reliability of the approach is to be questioned.

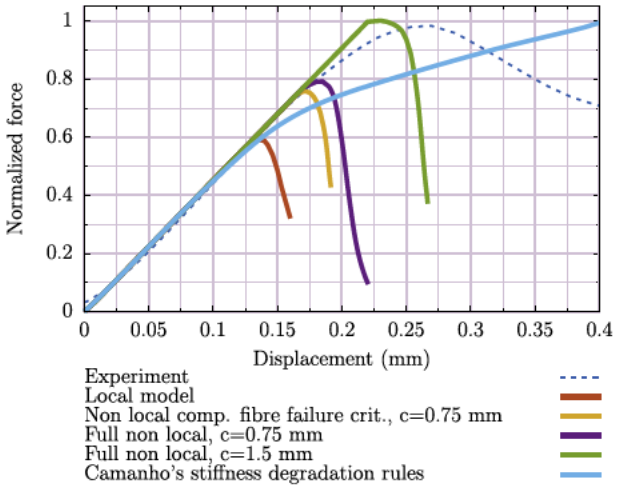

Fig. 14. Models vs typical experimental response. Note how conservative the local model is, and the effect of the internal length on the failure load. When only the compressive fibre failure criterion is computed in a non-local way, it is not possible to delay the final failure indefinitely by increasing the internal length. This is due to matrix damage, whose initiation remains local in this particular case.

Alternative non local approach. The delayed damage model is also a form of non local approach, although it does not explicitly introduce an internal length. Increasing the characteristic time τ while not using the implicit gradient enhanced model has an effect similar to that of the internal length. However, since the initiation remains local, it is possible to reproduce the non linear behaviour preceding the bearing peak (Fig. 15). A further analysis shows that the damaged zones fit those found in the CT analysis closely. How ever, increasing the characteristic time is not a reliable answer to

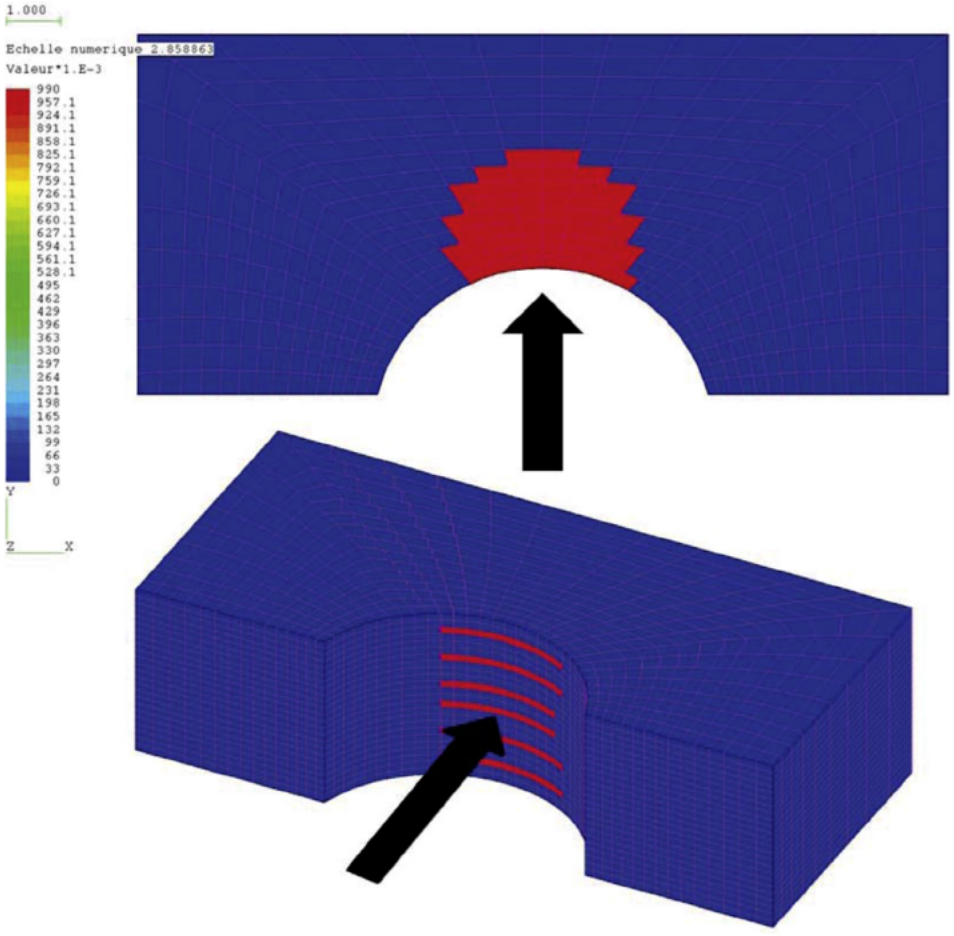

Fig. 13. Fibre compressive damage at bearing peak in a 0° ply (top), and global view of fibre compressive damage at bearing peak (bottom). Only 0° plies are damaged when the internal length is as large as 1.5 mm.

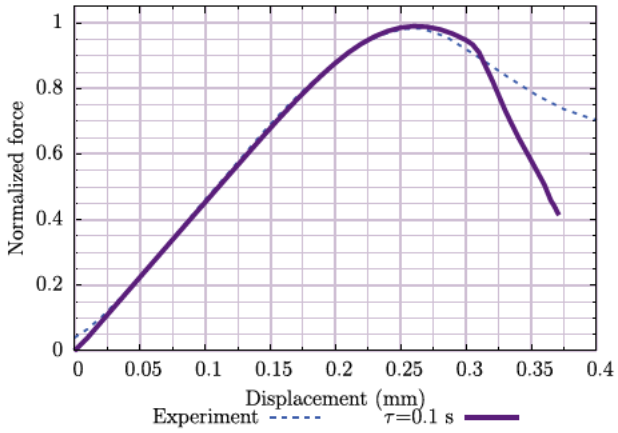

Fig. 15. Increasing the characteristic time constant τ in the delayed damage model makes it possible to obtain very good agreement between the typical experimental response and the model, up to the bearing peak at least.

the problem because it creates a strong dependence on the loading rate, and its physical meaning is rather unclear. It does, however, emphasise the need for progressive damage laws, since an increase in the characteristic time is equivalent to an increase in the failure energy density associated with each failure mode.

Although, after analysis of the CT scans, the non linear behaviour before the peak strength can clearly be related to progressive damage, up to now, no mention has been made of the non linear behaviours typically exhibited by composite laminates, namely shear non linearity, which is mainly due to the matrix, and compressive non linearity. The analysis of another model, proposed by Hochard and Thollon [27], showed that shear non linearity did not greatly influence the global behaviour of a quasi isotropic laminate loaded in bearing. Therefore, it would not explain the global non linearity. As to the non linear elastic behaviour of fibres loaded in compression, a previous numerical study based on Allix's model [28] concluded that it could not reasonably be held responsible for the observed non linearity. Using relevant parameters, the non linear behaviour would be too mild and would start at a much lower load than is actually the case.

To ensure a more reliable failure prediction, the failure model should become a proper damage model, with progressive failure laws associated with each damage mode, and specifically with fibre kinking, so as to make sure that the areas affected by the fibre compressive failure match the experimental observations.

Kinking is influenced by compressive as well as shear strains, as shown by Figs. 8 and 9. Therefore, a failure criterion of the maximum stress or strain type has little chance of providing completely meaningful results regarding the initiation of this damage mode. Although Pinho et al. [29] proposed a physically based failure criterion for kinking, it appears that this criterion is not fully satisfactory as new approaches based on fracture mechanics have recently been proposed by Pinho's coworkers Gutkin et al. [30] and Pimenta et al. [31]. In addition, a local version of this criterion would make the response of the model even more conservative, as $\pm 45°$ plies would fail at lower loads, their stress state being characterised by a combination of moderately high compressive and shear stresses, which are known to significantly affect the compressive strength. Should such a criterion be used, it would need to be non local, and the non linear behaviour of the matrix in shear would probably have to be taken into account, because it would have an effect on the criterion's value. When coupled with progressive failure laws, such a criterion would not need to be evaluated on a large volume to compensate for the lack of progressiveness of the damage laws, as is the case with the proposed model.

4. Conclusions

Bearing failure is a progressive structural failure which is itself the consequence of a progressive material failure dominated by the kinking phenomenon. The simple failure model proposed in this paper addresses structural failure by resorting to a progressive failure analysis, but disregards the progressiveness of the material failure. The non local approach applied to failure criteria and based on an empirical internal length does not seem sufficient to provide an adequate answer to the problem. Although it is obviously able to emulate the delaying effect progressive damage has on the peak strength at a macroscopic level, the local failure scenario is far too different from reality for this approach to be deemed reliable. Hence, the conclusion can be drawn that models based on traditional failure criteria, such as the model proposed in this paper, are unlikely to provide satisfactory results regarding bearing failure simulation. It appears that only physically based advanced numerical models could help reduce the excessive conservatism of simple engineering models, while providing sufficient reliability. However, these parameter intensive models require extensive material characterisation, which could also hamper their reliability should the parameter identification not be carried out properly. In addition, such models, based on a continuum damage mechanics framework, would probably not be able to simulate the effect of the wedge mechanisms, closely related to the crack nature of kink bands. Therefore, the proposed approach might still represent a good compromise at pre design stages, if the value of the internal length were to be confirmed by different bearing tests, making it more than a curve fitting parameter with little practical interest.

References

[1] Thoppul SD, Finegan J, Gibson RF. Mechanics of mechanically fastened joints in polymer-matrix composite structures - A review. Compos. Sci. Technol. 2009;69(3–4):301–29. http://dx.doi.org/10.1016/j.compscitech.2008.09.037.

[2] Van der Veen S, Bidaine B. Progressive failure analysis of the CFRP bearing test. In: Digimat users' meeting; 2013.

[3] Collings T. The strength of bolted joints in multi-directional CFRP laminates. Composites 1977;8(1):43–55.

[4] Kelly G, Hallström S. Bearing strength of carbon fibre/epoxy laminates: effects of bolt-hole clearance. Compos Part B: Eng 2004;35(4):331–43. http://dx.doi.org/10.1016/j.compositesb.2003.11.001.

[5] Xiao Y, Ishikawa T. Bearing strength and failure behavior of bolted composite joints (part I: experimental investigation). Compos Sci Technol 2005;65(7–8):1022–31. http://dx.doi.org/10.1016/j.compscitech.2005.02.011.

[6] Seike S, Takao Y, Wang W-X, Matsubara T. Bearing damage evolution of a pinned joint in CFRP laminates under repeated tensile loading. Int J Fatigue 2010;32(1):72–81. http://dx.doi.org/10.1016/j.ijfatigue.2009.02.010.

[7] Camanho P, Bowron S, Matthews F. Failure mechanisms in bolted CFRP. J Reinf Plast Compos 1998;17(3):205–33.

[8] Camanho PP, Matthews FL. A progressive damage model for mechanically fastened joints in composite laminates. J Compos Mater 1999;33(24):2248–80. http://dx.doi.org/10.1177/002199839903302402.

[9] Liu Y, Zwingmann B, Schlaich M. Nonlinear progressive damageanalysis of notched or bolted fibre- reinforced polymer (FRP) laminates based on a three-dimensional strain failure criterion. Polymers 2014;6(4):949–76. http://dx.doi.org/10.3390/polym6040949.

[10] Içten BM, Karakuzu R. Progressive failure analysis of pin-loaded carbon-epoxy woven composite plates. Compos Sci Technol 2002;62(9):1259–71.

[11] McCarthy C, McCarthy M, Lawlor V. Progressive damage analysis of multi-bolt composite joints with variable bolt-hole clearances. Compos Part B: Eng 2005;36(4):290–305. http://dx.doi.org/10.1016/j.compositesb.2004.11.003.

[12] Dano M-L, Kamal E, Gendron G. Analysis of bolted joints in composite laminates: strains and bearing stiffness predictions. Compos Struct 2007;79(4):562–70. http://dx.doi.org/10.1016/j.compstruct.2006.02.024.

[13] Wu PS, Sun CT. Modeling bearing failure initiation in pin-contact of composite laminates. Mech Mater 1998;29(3):325–35.

[14] Counts WA, Johnson WS. Bolt bearing fatigue of polymer matrix composites at elevated temperature. Int J Fatigue 2002;24(2):197–204.

[15] Ujjin R, Crosky A, Schmidt L, Kelly D, Li R, Carr D, Damage development during pin loading of a hole in a quasi-isotropic carbon fibre reinforced epoxy composite. In: Structural integrity and fracture international conference (SIF'04), 2004, pp. 359–365.

[16] Hirano N, Takao Y, Wang W-X. Effects of temperature on the bearing strength of CF/epoxy pinned joints. J Compos Mater 2006;41(3):335–51. http://dx.doi.org/10.1177/0021998306063374.

[17] Irisarri F-X, Laurin F, Carrere N, Maire J-F. Progressive damage and failure of mechanically fastened joints in CFRP laminates – Part I: refined finite element modelling of single-fastener joints. Compos Struct 2012;94(8):2269–77. http://dx doi org/10 1016/j compstruct 2011 07 023.
[18] Park H-J. Effects of stacking sequence and clamping force on the bearing strengths of mechanically fastened joints in composite laminates. Compos Struct 2001;53(2):213–21.
[19] Moran P, Liu X, Shih C. Kink band formation and band broadening in fiber composites under compressive loading. Acta Metall Mater 1995;43 (8):2943–58.
[20] Bažant ZP. Why continuum damage is nonlocal: micromechanics arguments. J Eng Mech 1991;117(5):1070–87.
[21] Hochard C, Lahellec N, Bordreuil C. A ply scale non-local fibre rupture criterion for CFRP woven ply laminated structures. Compos Struct 2007;80(3):321–6. http://dx.doi.org/10.1016/j.compstruct.2006.05.021.
[22] Bažant ZP, Kim J-JH, Daniel IM, Becq-Giraudon E, Zi G. Size effect on compression strength of fiber composites failing by kink band propagation. Fracture scaling. Springer; 1999. p. 103–41.
[23] Allix O, Feissel P, Thévenet P. A delay damage mesomodel of laminates under dynamic loading: basic aspects and identification issues. Comput Struct 2003;81(12):1177–91. http://dx.doi.org/10.1016/S0045-7949(03)00035-X.
[24] Gutkin R, Pinho S.T., In: Proceedings of the 18th international conference on composite materials, ICCM18, Jeju Island, Korea; 2011.
[25] Peerlings RHJ, Geers MGD, De Borst R, Brekelmans WAM. A critical comparison of nonlocal and gradient-enhanced softening continua. Int J Solids Struct 2001;38(44):7723–46.
[26] Germain N, Besson J, Feyel F. Composite layered materials: anisotropic nonlocal damage models. Comput Methods Appl Mech Eng 2007;196(41–44):4272–82. http://dx.doi.org/10.1016/j.cma.2007.04.009.
[27] Hochard C, Thollon Y. A generalized damage model for woven ply laminates under static and fatigue loading conditions. Int J Fatigue 2010;32(1):158–65. http://dx.doi.org/10.1016/j.ijfatigue.2009.02.016.
[28] Allix O, Ladeveze P, Vittecoq E. Modelling and identification of the mechanical behaviour of composite laminates in compression. Compos Sci Technol 1994;51(1):35–42.
[29] Pinho S, Iannucci L, Robinson P. Physically-based failure models and criteria for laminated fibre-reinforced composites with emphasis on fibre kinking: Part I: development. Compos Part A: Appl Sci Manuf 2006;37(1):63–73. http://dx.doi.org/10.1016/j.compositesa.2005.04.016.
[30] Gutkin R, Pinho S, Robinson P, Curtis P. A finite fracture mechanics formulation to predict fibre kinking and splitting in CFRP under combined longitudinal compression and in-plane shear. Mech Mater 2011;43(11):730–9. http://dx.doi.org/10.1016/j.mechmat.2011.08.002.
[31] Pimenta S, Gutkin R, Pinho S, Robinson P. A micromechanical model for kink-band formation: part II-analytical modelling. Compos Sci Technol 2009;69(7–8):956–64. http://dx.doi.org/10.1016/j.compscitech.2009.02.003.